

## Metasurface Polarization Optics: Independent Phase Control of Arbitrary Orthogonal States of Polarization

J. P. Balthasar Mueller, Noah A. Rubin, Robert C. Devlin, Benedikt Groever, and Federico Capasso\*

*John A. Paulson School of Engineering and Applied Sciences, Harvard University, Cambridge, Massachusetts 02138, USA*

(Received 22 June 2016; published 14 March 2017)

We present a method allowing for the imposition of two independent and arbitrary phase profiles on any pair of orthogonal states of polarization—linear, circular, or elliptical—relying only on simple, linearly birefringent wave plate elements arranged into metasurfaces. This stands in contrast to previous designs which could only address orthogonal linear, and to a limited extent, circular polarizations. Using this approach, we demonstrate chiral holograms characterized by fully independent far fields for each circular polarization and elliptical polarization beam splitters, both in the visible. This approach significantly expands the scope of metasurface polarization optics.

DOI: 10.1103/PhysRevLett.118.113901

Metasurfaces, subwavelength arrays of optical phase-shifting elements, provide an exciting platform for ultrathin optics [1]. A distinguishing feature of metasurfaces is the sophistication with which the individual phase-shifting elements can be engineered. In particular, metasurface elements can be designed to impart distinct phases on orthogonal linear polarizations. Such elements can then be described by the Jones matrix of a conventional, *linearly birefringent* wave plate [2]:

$$J = R(-\theta) \begin{bmatrix} e^{i\phi_x} & 0 \\ 0 & e^{i\phi_y} \end{bmatrix} R(\theta). \quad (1)$$

Here, the element imposes phase shifts  $\phi_x$  and  $\phi_y$  on light linearly polarized along its fast and slow axes which are rotated by an angle  $\theta$  relative to the reference coordinate system ( $R$  is a  $2 \times 2$  rotation matrix). This wave-plate-like behavior could be realized with, for example, plasmonic antennas [1], liquid crystals [3] (which, due to their size cannot truly be considered metasurface elements), or waveguide-like dielectric pillars exhibiting mode birefringence fabricated from Si [4–6], GaAs [7], or TiO<sub>2</sub> [8,9] with, e.g., an elliptical or rectangular cross section.

A metasurface composed of these linearly birefringent elements can then act as a different optical element depending on the polarization of incident light. From a technological standpoint, this exciting capability allows for a new class of polarization-switchable optical components.

Previously, metasurfaces imparting polarization-dependent phase have fallen into two categories: (1) Propagation phase designs, which allow for the imposition of independent and arbitrary phase profiles on each of two orthogonal, *linear* polarizations and (2) Geometric (or Pancharatnam-Berry) phase designs, which allow for metasurfaces imparting *equal and opposite* phase profiles on the two circular polarizations. We describe each of these strategies below.

Crucially, neither propagation nor geometric phase designs alone are able to address elliptical polarizations, representing the most general case. Intuitively, it is unclear whether this should even be possible with only simple, linearly birefringent wave plate elements which, after all, only distinguish between linear polarizations. In this work, we show that the geometric and propagation phases used in tandem allow for the imposition of arbitrary phase profiles on any two orthogonal polarization states (linear, circular, or elliptical), significantly expanding the scope of metasurface polarization optics and allowing for new polarization-switchable metasurfaces.

We begin by considering the propagation phase alone. At each point on a metasurface, the characteristic phase shifts  $\phi_x$  and  $\phi_y$  imposed by an element can be individually tailored by adjusting its shape while its angular orientation  $\theta$  is held fixed. In this way, arbitrary and independent spatial phase profiles can be imposed on any set of orthogonal, linear polarizations using the so-called propagation (or dynamical) phase [Fig. 1(a)] [10]. Using this approach, for instance, a single metasurface could act as a lens for  $x$ -polarized light and encode a hologram for  $y$ -polarized light [5].

The propagation phase is one of two means of imposing polarization-dependent phase [11]. The other, the geometric phase, stems from polarization change. Specifically, if two parts of a uniformly polarized wave front are transported to a common polarization state along two different paths on the Poincaré sphere (polarization state space), a relative phase emerges between the two equal to half the solid angle enclosed by the path [12]. Less abstractly, this effect can be harnessed to attain metasurfaces sensitive to circular polarizations. A metasurface composed of half-wave plate elements ( $|\phi_x - \phi_y| = \pi$ ) whose angular orientations  $\theta(x, y)$  vary over its spatial extent imposes a phase profile on one of the circular polarizations equal to  $\phi(x, y) = 2\theta(x, y)$  [Fig. 1(b)]. These

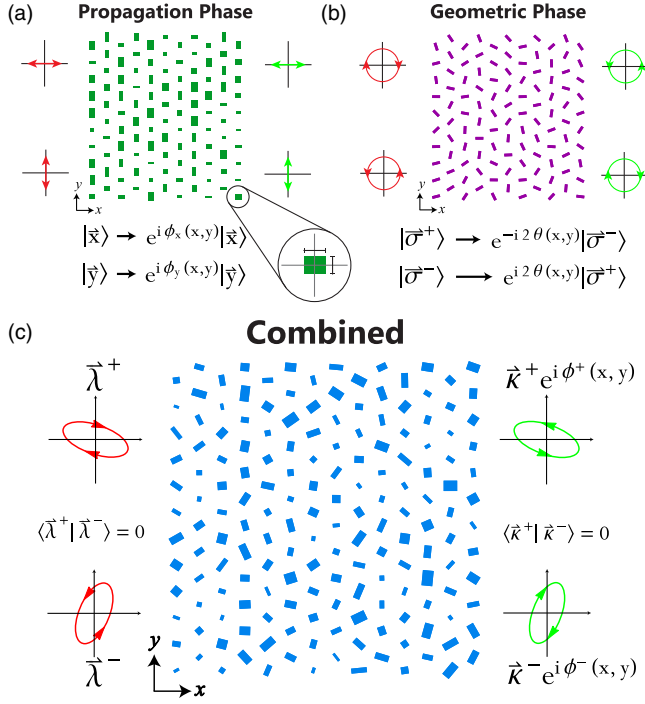


FIG. 1. Conceptual schematic. (a) At each point  $(x, y)$  on a metasurface, the dimensions of a wave plate-like shape-birefringent element (inset) can be varied to impose unique phases  $\phi_x$  and  $\phi_y$  on light linearly polarized along each axis. In this approach, which employs the propagation phase alone, element dimensions are varied while the orientation angle  $\theta$  is held fixed. When each of two *orthogonal, linear* input polarizations (red, on left) are incident, arbitrary, and independent phase profiles,  $\phi_x(x, y)$  and  $\phi_y(x, y)$  can be imparted upon each; the output states (green, on right) are unconverted. (b) Using the geometric phase alone, phase profiles of *equal* and *opposite* magnitude can be imparted on the two *circular* polarizations. If elements with half-wave ( $\pi$ ) retardance are rotated at angles  $\theta(x, y)$  at each point, one input circular polarization (red, on left) will pick up a phase of  $2\theta(x, y)$  and the other  $-2\theta(x, y)$  with each changing handedness upon reflection or transmission (green, on right). Here, element dimensions are fixed and the orientation  $\theta$  is varied. (c) By varying both element dimensions and  $\theta$  over the extent of the metasurface—that is by combining the geometric and propagation phases—we show that arbitrary and independent phase profiles  $\phi^\pm(x, y)$  can be imparted on any set of orthogonal input states  $\vec{\lambda}^\pm$  (red, on left). Each must flip handedness upon reflection or transmission (green, right).

retarders convert right-circularly polarized (RCP) [left-circularly polarized (LCP)] light to LCP [RCP] light along a state-space path determined by the element's orientation, yielding a geometric phase that increases linearly from 0 to  $2\pi$  as the element is rotated at angles from 0 to  $\pi$ . If, however, the phase profile imposed in this way on RCP light is some  $\phi_{\text{RCP}}(x, y)$ , the phase profile imparted on a LCP wave front is automatically  $\phi_{\text{LCP}}(x, y) = -\phi_{\text{RCP}}(x, y)$ . This restriction—an inherent symmetry of the geometric phase—still allows for, e.g., circular polarization beam

splitters that deflect opposite circular polarizations by equal and opposite angles [4,13,14], but has important practical consequences: a geometric phase converging lens for one circular polarization, for example, will act as a diverging lens for the other [15].

We now show that using a single layer of birefringent metasurface elements, one can indeed impose arbitrary and independent phase profiles on any set of orthogonal polarizations by combining the propagation and geometric phases [Fig. 1(c)], the only restriction being that the handedness of each polarization is flipped upon interaction with the metasurface. In contrast to previous designs using propagation or geometric phase alone, this allows for metasurfaces imparting fully independent phase profiles separately on each of any two orthogonal polarizations (including circular and elliptical).

Let the orthogonal polarization states upon which the metasurface should impart independent phase profiles be given by orthogonal Jones vectors  $\vec{\lambda}^+ = \begin{bmatrix} \lambda_1^+ \\ \lambda_2^+ \end{bmatrix}$  and  $\vec{\lambda}^- = \begin{bmatrix} \lambda_1^- \\ \lambda_2^- \end{bmatrix}$ . The output wave front corresponding to each input polarization state  $\{\vec{\lambda}^+, \vec{\lambda}^-\}$  should have homogenous polarization, so we require that the metasurface consistently transforms the input polarization states to output polarization states  $\{\vec{\kappa}^+, \vec{\kappa}^-\}$  as  $\vec{\lambda}^+ \rightarrow \vec{\kappa}^+$  and  $\vec{\lambda}^- \rightarrow \vec{\kappa}^-$  over its entire spatial extent. Suppose we are interested in designing a metasurface imposing arbitrary spatial phase profiles  $\phi^\pm(x, y)$  on the states  $\vec{\lambda}^\pm$ . That is, at each point  $(x, y)$  we require a metasurface element whose Jones matrix  $J(x, y)$  simultaneously satisfies

$$J(x, y)\vec{\lambda}^+ = e^{i\phi^+(x, y)}\vec{\kappa}^+ \quad (2)$$

and

$$J(x, y)\vec{\lambda}^- = e^{i\phi^-(x, y)}\vec{\kappa}^-. \quad (3)$$

This treatment is justified because each element is assumed to be much smaller than the illuminating beam, so that it experiences plane wavelike light. Mathematically, the above system [Eqs. (2) and (3)] is solvable for any choice of  $\{\vec{\kappa}^+, \vec{\kappa}^-\}$ . However, restricting ourselves to a single layer of metasurface elements with linear structural birefringence,  $J$  is constrained to the form of Eq. (1). It can be shown that this constraint directly implies that the output polarization states  $\{\vec{\kappa}^+, \vec{\kappa}^-\}$  must be the same states as the input states  $\{\vec{\lambda}^+, \vec{\lambda}^-\}$  with flipped handedness—mathematically,  $\vec{\kappa}^\pm = (\vec{\lambda}^\pm)^*$  where  $*$  denotes the complex conjugate. The reason for this follows intuitively from the physics of wave plates (a simple geometrical argument is detailed in the Supplemental Material [16]).

Given this knowledge of  $\{\vec{\kappa}^+, \vec{\kappa}^-\}$ , the original system can be recast as

$$J(x, y) = \begin{bmatrix} e^{i\phi^+(x,y)}(\lambda_1^+)^* & e^{i\phi^-(x,y)}(\lambda_1^-)^* \\ e^{i\phi^+(x,y)}(\lambda_2^+)^* & e^{i\phi^-(x,y)}(\lambda_2^-)^* \end{bmatrix} \begin{bmatrix} \lambda_1^+ & \lambda_1^- \\ \lambda_2^+ & \lambda_2^- \end{bmatrix}^{-1}. \quad (4)$$

Requiring  $\vec{\kappa}^\pm = (\vec{\lambda}^\pm)^*$  here guarantees that the Jones matrix  $J(x, y)$  at each point  $(x, y)$  represents a linearly birefringent wave plate [in the sense of Eq. (1)]. By specifying the desired phase shifts  $\phi^\pm$  and target states  $\vec{\lambda}^\pm$ ,  $J$  is determined by Eq. (4). Being linearly birefringent, the  $J$  so obtained has eigenpolarizations which are orthogonal and linear on which it imparts characteristic phase shifts  $\{\phi_x, \phi_y\}$ . The geometry of an element imposing these required phase shifts on the linear eigenpolarizations can be located with, e.g., finite difference time domain (FDTD) simulation; the orientation of the linear eigenpolarizations determine the element's fast and slow axes and thus the orientation angle  $\theta$ .

In summary, a physical metaelement imparting phases  $\phi^\pm$  on arbitrary orthogonal polarization states  $\vec{\lambda}^\pm$  has a Jones matrix  $J$  defined by Eq. (4); the orientation and dimensions of an element implementing this  $J$  are then determined by the angle of  $J$ 's orthogonal linear eigenpolarizations and the characteristic phase shifts  $\{\phi_x, \phi_y\}$  imposed upon them. It should be noted that this possibility was recognized in the supplementary information to Ref. [5] where it was, however, described only briefly and from a purely theoretical standpoint.

The above result can be understood as a unification of the propagation and geometric phases in a single element. Desired phases can be imparted on any set of orthogonal polarization states by modifying an element's shape birefringence and angular orientation simultaneously [Fig. 1(c)].

To demonstrate this arbitrary phase control for polarizations other than linear polarizations, we designed, fabricated and tested a metasurface encoding separate holograms for RCP and LCP light. The near-field phase profiles yielding far-field intensity images of a cartoon cat and dog were computed using iterative phase retrieval [18] and a metasurface consisting of noninteracting, elliptical  $\text{TiO}_2$  pillars was designed to impose these phase profiles independently on each circular polarization in transmission. Here a broad range of pillars (with semi-major and minor axes ranging from 50–300 nm, all assuming a height of 600 nm set by our fabrication process) was simulated using full-wave FDTD simulations to find those that would satisfy the phase-shifting properties solved for in Eq. (4) [16]. Fabricated with a recently reported  $\text{TiO}_2$  process on glass [8], the pillars were arranged in a square lattice with 500 nm nearest-neighbor separation [Figs. 2(b) and 2(c)]. The metasurface was designed for and tested in the visible at  $\lambda = 532$  nm. The measured far-field intensity profiles upon illumination with each circular polarization matched the design images with significant detail [Fig. 2(a)]. Slight differences between the design images and measured

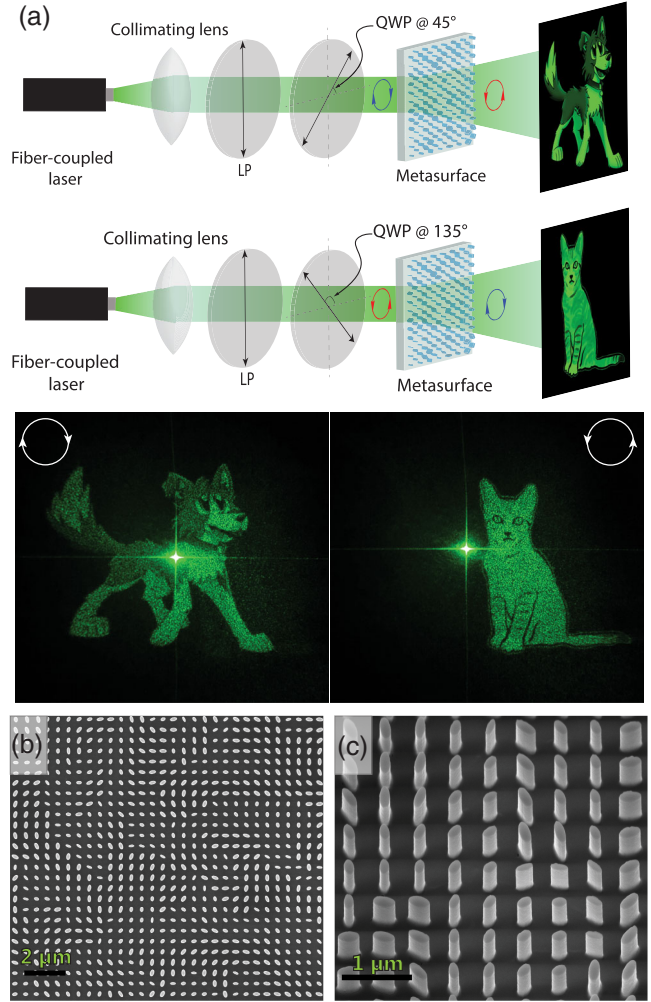


FIG. 2. Chiral Holograms. (a) A single metasurface encodes two independent hologram phase profiles for each circular polarization at  $\lambda = 532$  nm. When illuminated with RCP (LCP), the metasurface projects an image of a cartoon dog (cat) to the far field. Design images are shown in the schematic (top) and measured projections on a screen are shown below. The dog (cat) occupies  $17^\circ$  ( $15^\circ$ ) of arc. The bright dot in the center of each represents zero-order light not coupling into the metasurface due to fabrication imperfections and beam overfilling. (b) The metasurface encoding these holograms was  $350 \times 300 \mu\text{m}$  in size and contained 420 000  $\text{TiO}_2$  pillars of elliptical cross section. Shown is an SEM of the device. (c) Oblique view.

holograms shown in Fig. 2(a) are attributable to fabrication imperfections and an assumption by the phase reconstruction algorithm of uniform amplitude transmission at each point  $(x, y)$ . It should be noted that while metasurface chiral holograms for circular polarizations have been reported [19,20], the phase profiles imparted on each circular polarization, and thus the projected far fields, are not fully independent due to a reliance on geometric phase alone. In these cases, only sections of the far field (such as individual diffraction orders) can contain independent images for each chirality. Using the

method presented here, the phase profiles imparted on each circular polarization—and, consequently, the resulting far fields—can be completely decoupled.

Metasurfaces acting as polarization beam splitters (i.e., blazed gratings deflecting light in a direction dependent on its polarization) have been demonstrated extensively for orthogonal linear polarizations using propagation phase (where the deflection angles can be arbitrary) [5,21,22] and for circular polarizations using the geometric phase (where the deflection angles are constrained to be equal and opposite) [3,4,13,14,21], though never for elliptical polarizations. This has consequences especially for polarimetry, where a thorough sampling of polarization state space, including elliptical states, is necessary to optimize sensitivity [23–25]. We demonstrate here elliptical polarization beam splitters, a novel class of optical components.

A metasurface deflecting light at an angle  $\beta$  must impose a linear phase profile given by  $(2\pi x/\lambda)\sin\beta$  with  $x$  the spatial coordinate along the splitting direction [1]. A metasurface polarization beam splitter, then, must impose two such phase profiles with different  $\beta$  on each of two polarizations. Using the geometric and propagation phases in tandem as described above, this is possible for any set of two orthogonal, elliptical polarizations. To showcase this capability, we designed six such beam-splitting metasurfaces for six different sets of elliptical polarizations, each of which was designed to deflect orthogonal polarizations at  $\pm 7^\circ$  (though we stress that the angles are not constrained to be equal or opposite with this method). The elliptical polarizations chosen—the “split states”—were the six sets of orthogonal Stokes vectors matching the vertices of a regular icosahedron inscribed in the Poincaré sphere (Fig. 3). The choice of an icosahedron in particular, and the platonic solids in general, corresponds to optimal sampling of states for polarimetry [25].

The geometry of each beam-splitter unit cell, along with the polarization ellipses of the split states, are shown in Fig. 3(a). These were realized with 600 nm high rectangular  $\text{TiO}_2$  pillars whose lateral dimensions ranged from 50–250 nm, on a hexagonal grid with 420 nm nearest-neighbor separation. The unit cells shown (Nos. 1–6) were tessellated to form six different metasurfaces, each  $300 \times 300$  microns in size. The testing of each metasurface beam splitter involved illumination with a set of six test polarization states. By measuring the  $m = \pm 1$  diffraction order intensity in response to each, the polarization states to which the device is most selective (i.e., the states of polarization for which the extinction ratio between orders is maximized) were obtained [26]; ideally, these would match the designed split states. In Fig. 3(b), these states of maximal selectivity are plotted on the Poincaré sphere alongside the designed split states, showing good agreement. The same data are presented in graphical form in Fig. 3(c). Discrepancy between the design and measured states can be attributed to imperfections in the fabricated

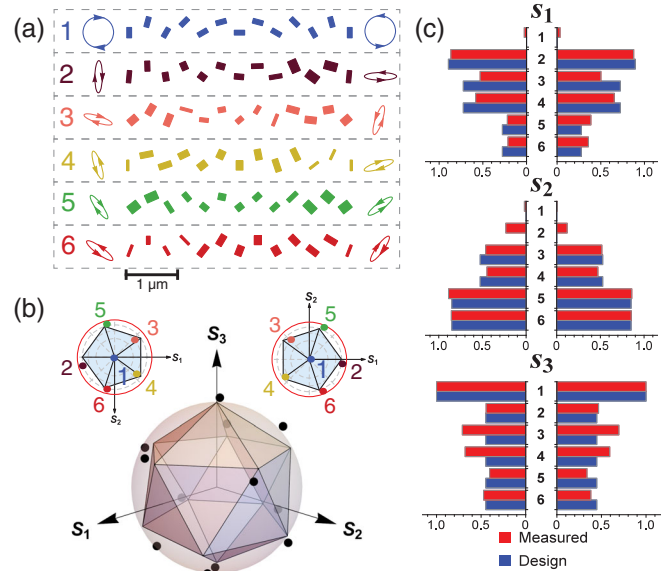


FIG. 3. Elliptical polarization beam splitters. (a) A metasurface imposing a linear spatial phase gradient will deflect normally incident light at an angle. A metasurface imposing phase gradients with different slopes on different polarizations will function as a polarization beam splitter. Using the formalism presented, six metasurface beam splitters (each  $300 \times 300 \mu\text{m}$  in size) whose unit cells are shown were designed to split six sets of orthogonal, elliptical polarizations (the split states) at  $\lambda = 532 \text{ nm}$ . The polarization ellipses of these split states are shown on either side of each corresponding unit cell. Note that No. 1 is a conventional geometric phase grating for circular polarizations, but that designs No. 2–6 represent new functionality. (b) The six sets of orthogonal split states shown in (a) have Stokes states of polarization (SOP) defined by the vertices of a regular icosahedron inscribed in the Poincaré sphere. The northern (top right) and southern (top left) hemispheres of the sphere are shown. Each metasurface (Nos. 1–6) was illuminated with a set of test polarization states and the intensities on the  $\pm 1$  diffraction orders in response to each were measured and used to compute the actual split SOPs. These are shown as black dots on the Poincaré sphere (center) and color-coded, numbered dots on each hemisphere, showing good agreement with the design SOPs (vertices). (c) The same data, presented as bar charts of the Stokes coordinates ( $s_1, s_2, s_3$ ).

sizes of the elements. A more detailed description of this beam-splitter characterization is deferred to the Supplemental Material [16].

In summary, we demonstrate here how a broad class of metasurfaces can impose arbitrary and independent phase profiles on any set of orthogonal polarization states, notably extending this capability to chiral polarizations without relying on chiral birefringence. We show in particular how this ability can be used to target elliptical polarization states, and provide an intuition for this phenomenon as arising from the combination of propagation and geometric phase. This formalism generalizes the design space offered by polarization-sensitive, linearly birefringent metasurfaces, enabling polarization switchable

lenses for chiral polarizations, more versatile  $q$  plates, and improved metasurface polarimeters (to name a few examples), illustrating further that metasurfaces represent a uniquely powerful platform for polarization optics.

The authors wish to acknowledge Lulu Liu (Harvard University) who was of great help in capturing high-quality images of the holograms and Tobias Mansuripur (Harvard University) for helpful comments. This work was supported in part by the Air Force Office of Scientific Research (MURI, Grants No. FA9550-14-1-0389 and No. FA9550-16-1-0156). Additionally, N. A. R. is supported by the NSF Graduate Research Fellowship Program (GRFP) under Grant No. DGE1144152. R. C. D. acknowledges support from a fellowship through Charles Stark Draper Laboratory. This work was performed in part at the Center for Nanoscale Systems (CNS), a member of the National Nanotechnology Coordinated Infrastructure (NNCI), which is supported by the National Science Foundation under NSF award No. 1541959. CNS is part of Harvard University.

J. P. B. M. and N. A. R. contributed equally to this work.

---

\*capasso@seas.harvard.edu

- [1] N. Yu, P. Genevet, M. A. Kats, F. Aieta, J. P. Tetienne, F. Capasso, and Z. Gaburro, *Science* **334**, 333 (2011).
- [2] B. E. Saleh and M. C. Teich, *Fundamentals of Photonics*, 2nd ed. (Wiley-Interscience, New York, 2007).
- [3] C. Oh and M. J. Escuti, *Opt. Lett.* **33**, 2287 (2008).
- [4] D. Lin, P. Fan, E. Hasman, and M. L. Brongersma, *Science* **345**, 298 (2014).
- [5] A. Arbabi, Y. Horie, M. Bagheri, and A. Faraon, *Nat. Nanotechnol.* **10**, 937 (2015).
- [6] Y. Yang, W. Wang, P. Moitra, I. I. Kravchenko, D. P. Briggs, and J. Valentine, *Nano Lett.* **14**, 1394 (2014).
- [7] Z. Bomzon, V. Kleiner, and E. Hasman, *Opt. Lett.* **26**, 1424 (2001).
- [8] R. C. Devlin, M. Khorasaninejad, W.-T. Chen, J. Oh, and F. Capasso, *Proc. Natl. Acad. Sci. U.S.A.* **113**, 10473 (2016).
- [9] M. Khorasaninejad, W. T. Chen, R. C. Devlin, J. Oh, A. Y. Zhu, and F. Capasso, *Science* **352**, 1190 (2016).
- [10] M. Berry, *Proc. R. Soc. A* **392**, 45 (1984).
- [11] M. J. Escuti, J. Kim, and M. W. Kudenov, *Opt. Photonics News* **27**, 22 (2016).
- [12] S. Pancharatnam, *Proc. Indian Acad. Sci. A* **44**, 247 (1956).
- [13] E. Hasman, Z. Bomzon, A. Niv, G. Biener, and V. Kleiner, *Opt. Commun.* **209**, 45 (2002).
- [14] M. Khorasaninejad and K. B. Crozier, *Nat. Commun.* **5**, 5386 (2014).
- [15] E. Hasman, V. Kleiner, G. Biener, and A. Niv, *Appl. Phys. Lett.* **82**, 328 (2003).
- [16] See Supplemental Material at <http://link.aps.org/supplemental/10.1103/PhysRevLett.118.113901> for further theoretical and experimental detail, which includes Ref. [17].
- [17] J. N. Damask, *Polarization Optics in Telecommunications* (Springer, New York, 2005).
- [18] R. W. Gerchberg and W. O. Saxton, *Optik (Stuttgart)* **35**, 237 (1972).
- [19] D. Wen, F. Yue, G. Li, G. Zheng, K. Chan, S. Chen, M. Chen, K. F. Li, P. W. Wong, K. W. Cheah, E. Y. Pun, S. Zhang, and X. Chen, *Nat. Commun.* **6**, 8241 (2015).
- [20] M. Khorasaninejad, A. Ambrosio, P. Kanhaiya, and F. Capasso, *Sci. Adv.* **2**, e1501258 (2016).
- [21] A. Pors, O. Albrektsen, I. P. Radko, and S. I. Bozhevolnyi, *Sci. Rep.* **3**, 2155 (2013).
- [22] A. Pors and S. I. Bozhevolnyi, *Opt. Express* **21**, 27438 (2013).
- [23] A. Pors, M. G. Nielsen, and S. I. Bolzhevolnyi, *Optica* **2**, 716 (2015).
- [24] J. S. Tyo, *Appl. Opt.* **41**, 619 (2002).
- [25] D. S. Sabatke, M. R. Descour, E. L. Dereniak, W. C. Sweatt, S. A. Kemme, and G. S. Phipps, *Opt. Lett.* **25**, 802 (2000).
- [26] J. P. B. Mueller, K. Leosson, and F. Capasso, *Nano Lett.* **14**, 5524 (2014).